A DFT study of formation energies of Fe-Zn-Al intermetallics and solutes

Klaver, TPC; Madsen, GKH; Drautz, R

DOI
https://doi.org/10.1016/j.intermet.2012.06.017

Publication date
2012

Document Version
Accepted author manuscript

Published in
Intermetallics

Citation (APA)
Klaver, TPC., Madsen, GKH., & Drautz, R. (2012). A DFT study of formation energies of Fe-Zn-Al intermetallics and solutes. *Intermetallics*, *31*, 137-144. https://doi.org/10.1016/j.intermet.2012.06.017

. published in Intermetallics 31 (2012) p137–144

A DFT study of formation energies of Fe-Zn-Al intermetallics and solutes

T. P. C. Klaver[1, 2*], G. K. H. Madsen[1], R. Drautz[1]

[1] Interdisciplinary Centre for Advanced Materials Simulation, Ruhr-Universität Bochum, Germany
[2] Department of Materials Science and Engineering, Delft University of Technology, Mekelweg 2, 2628 CD Delft, The Netherlands.

Abstract

We report Density Functional Theory results on FeAl and FeZn intermetallics and Fe, Zn and Al solute atoms. The formation energies of fully relaxed intermetallic geometries were determined, as well as solution energies of the three elements in host lattices of the other two elements. Since it is know that the outcome of the magnetic states of some FeAl intermetallics and Fe solutes in Al depends on subtle details of how the calculations are carried out, we have determined many of our results with two different parameterisations, PBE and PBEsol, so see how the parameterisation influences the results.
The relaxed intermetallic geometries are in good agreement with experimental results, with PBEsol calculations resulting in slightly smaller geometries than PBE calculations (0.7 - 2.1%). Intermetallic formation energies fall within ranges of experimental results where available, and are in excellent or reasonable agreement with other DFT results, except for the $FeAl_2$ phase. For this phase a structure revision was recently suggested and the heat of formation of the newly suggested structure is 0.1 eV/atom lower than for the long-accepted structure. The formation energies of Fe aluminides are an order of magnitude more negative than those of FeZn intermetallics. Most of the calculated magnetic states of the intermetallics are at odds with experimental results. However, the intermetallic formation energies are often not strongly affected by this.
Fe/Al solute systems have the most negative solution energies. All other solution energies are positive and smaller in absolute value than the Fe/Al solution energies. Solution energies were all some tenths of eV. Where comparisons could be made, calculated and experimental results differed by some hundredths of eV. The magnetic moment found on an Fe solute in Al is at odds with experimental results. As with FeAl, the outcome of the magnetic state subtly depends on the details of how calculations were performed and has little energetic effect. Lattice relaxation around solute atoms is mostly in agreement with simple atomic size considerations. The slight relaxation of Al neighbours away from a Zn solute is at odds with this pattern, and also with experimental results.

Keywords: A iron aluminides; A ternary alloy systems; B thermodynamic and thermochemical properties; E ab-initio calculations; E phase stability, prediction

1. Introduction

Hot dip galvanising is a technique that has been used for a long time to cover steel parts with a protective layer. The process offers a relatively cheap and easy way of protecting parts that, due to the fact that Zn is less ‘noble’ than Fe, remains effective even after some of the Zn has dissolved or has been removed due to wear. Yet despite its long history of application, the process is today still partly empirical in nature. One improvement to the process of simply dipping steel parts into molten Zn is the addition of small amounts of aluminium to the Zn bath. Without aluminium, part of the coating that results from hot dipping will consist of FeZn intermetallics, see e.g. [1]. These are hard and brittle, which makes them crack and flake off easily under deformation. They have other undesirable qualities too, such as relatively poor corrosion properties and an unattractive appearance. When some aluminium is added to the Zn bath, it forms a film of Fe aluminides, see e.g. [2], that mostly prevents contact between the steel and the molten Zn. This temporarily prevents FeZn intermetallic formation until Zn ‘outburst’ occurs [3]. This process is certainly not rigourously understood to a level where the occurrence of the different phases present can be accurately predicted. The process involves a complex system not in equilibrium. It involves some solution of elements into each other, quickly followed by the formation of a range of intermetallic compounds. Instead of forming the most stable compound straight away, the compounds may transition into each other with time, and require more diffusion along the way to do so. Even predicting the phases and their amounts present in equilibrium would require knowing the Gibbs free energy of the different phases as a function of temperature and also as a function of composition for some, as some of the intermetallics are stable over a range of compositions around their stoichiometry point (possibly involving some solution of the third element in an intermetallic of the other two) [4, 5, 6]. For some of the phases involved only the formation enthalpy of the compounds at their stoichiometry composition is available and we were unable to find solution energies for some of the Fe-Zn-Al element combinations.

Part of the interest in Fe aluminides stems from the practical applications that some of them have, e.g. in (high temperature) sulfidation, aqueous corrosion and oxidation environments, as a cheaper alternative to stainless steel or for weight saving considerations. Examples of other specific applications include use as heating elements (thanks to their high electrical resistivity) and diffusion barrier coatings [7]. Fe aluminides have some poor mechanical properties, including brittleness, but heat treatments and alloying with various elements has been used to improve them [8]. Even if not wanted for an application in its own right, Fe aluminides can also appear when Fe and Al are combined through welding in e.g. the automotive industry. They can cause cracking in the joining zone [5] and are therefore not wanted, but still of practical relevance.

From an electronic structure modelling point of view one of the aluminides, α_2 FeAl, has been the subject of considerable debate. While experimentally α_2 FeAl is know not to be magnetic, some DFT calculations did result in magnetic solutions. The system appears to be near a tipping point where obtaining a magnetic or non-magnetic outcome hinges on details of how calculations are performed, see e.g. [9].

For Fe aluminides a considerable number of studies of the formation enthalpies have been reported, using experiment, Density Functional Theory (DFT) or CALPHAD-type or other thermodynamic assessment [6, 10-19, references in 13, 19]. Formation enthalpies reported both from experiments and DFT studies have varied considerably. For example, for the α_1 Fe_3Al phase, experimental formation energies have been reported ranging from -0.15 to -0.32 eV/atom and there is even disagreement between different DFT methods as to what the most stable crystal structure is [21]. Only one very recent DFT study [17] that appeared during the writing stages of our study reported values for all Fe aluminides. However, the study did not include FeZn intermetallics or solutes. Given the variation in the values reported and contradictions in DFT results, combining values from different studies would not even always result in the same order of stability of the various phases.

In contrast to the many and varied Fe aluminide results, Reumot *et al* [20] noted the shortage of thermodynamic data for the FeZn system.

Obviously, it would be useful to have one consistent set of formation and solution energies determined with a similar method and similar settings. Assuming that errors would be mostly consistent between the results for different phases, at least the relative stability of the different phases would be more reliable than from the data presently available from different sources. We have carried out a DFT study to determine the formation energies of most of the FeAl and FeZn intermetallic phases that occur in the galvanising process. Since for some intermetallics the outcome of DFT calculations depends on subtle details of how the calculations were performed, we have run most of our calculations with two different functionals to see if the calculations would result in different outcomes concerning the magnetic state, and if so, how much difference in formation or solution energy this makes. The results reported in this paper are the first milestone in our more extensive plans to also determine the formation energies of ternary compounds, include Mn alloying and look at relevant (mixed) Fe-Zn-Al-Mn oxides involved.

2. Computational details

Results were calculated using the DFT package VASP v5.2 [22, 23]. VASP is a plane wave code that implements the PAW method [24, 25]. The standard PAW potentials supplied with VASP were used. Exchange and correlation were described by the PBE parameterization or the PBE parameterization adapted for solids (PBEsol [26]), both in the generalized gradient approximation. Treating Fe semi-core states as valence electrons proved not to have significant effects on our results, and hence an Fe potential with 8 valence electrons was used. Al and Zn potentials had 3 and 12 valence electrons. A 400 eV plane wave energy cut-off was used and it was verified that this was enough for absolute energy convergence. For intermetallics, cell shapes and volumes and internal atom coordinates were relaxed. Force components on atoms were relaxed to less than 0.01 eV/Å and normal stresses were relaxed to less than 0.25 MPa. After relaxations involving cell shape or volume changes, the systems were recalculated with a newly determined plane wave basis set to obtain accurate total energies. Brillouin zone sampling was done using the Monkhorst–Pack

scheme. For a 2-atom bcc Fe unit cell a sampling of 20^3 k-points was used, for other cells spacings were used that were approximately as fine. Given the fine k-point sampling in all calculations, no special attention was paid to always using or always avoiding Γ-centred k-point grids. Magnetic moments were evaluated in spheres around nuclei. For Fe, Al and Zn the sphere radii were 1.302, 1.402 and 1.270 Å. Since the choice of radii can influence the outcome of the moments evaluation, trends in the moments are probably quite reliable but absolute values may have some error bar on them.
The 0 K formation energy E_f of a system of n atoms of element A and m atoms of element B is calculated as

$$E_f = E(A_nB_m) - nE_A - mE_B \tag{1}$$

where $E(A_nB_m)$ is the calculated total energy for the system and E_A and E_B are the energies per atom of elements A and B in their reference state, i.e. in the low temperature crystal structure at equilibrium lattice spacing.
The solution energy E_b of element A in B is simply the formation energy of a single solute of element A in a large system of element B. Throughout this paper formation energies are expressed in eV/atom and solution energies in eV/solute. For solute systems 3x3x3 k-points used without checking if that is sufficient for absolute energy convergence and some other precision-related parameters were set lower than for intermetallics as well. Also, these calculations were done at fixed equilibrium volume rather than at zero pressure. This might seem to go against the idea of having all results calculated with similar settings. However, the large solute systems are very similar to the related large pure element systems used for reference. Hence cancellation of systematic errors means that the results would not be very different if they were calculated at higher precision settings. Given the relatively large size of the solute systems, the equilibrium volume vs. zero pressure difference is also not very important.

3. Results and discussion

3.1. Intermetallic phases studied, phase diagrams

As part of his discussion of the FeZnAl ternary system, Gosh [27] includes a table of 11 intermetallic phases. It contains six FeAl intermetallics (α_1 Fe_3Al, α_2 FeAl, ε Fe_5Al_8 [28], $FeAl_2$, η Fe_2Al_5 (the main constituent of the Fe aluminide inhibitor film between Fe and the Zn bath) and Fe_4Al_{13} (also found in the inhibitor film), the last in that list is sometimes also referred to as $FeAl_3$), 4 FeZn intermetallics (Γ Fe_3Zn_{10} (Zhou *et al* put the composition as Fe_4Zn_9 [29]), Γ_1 $Fe_{11}Zn_{39}$ (often noted as $Fe_{11}Zn_{40}$ or Fe_5Zn_{21} by others), δ $FeZn_{10}$ and ζ $FeZn_{13}$) and the ternary Γ_2 intermetallic. It should be noted that some authors have deviated from the naming conventions commonly used to denote FeZn intermetallics. The phases referred to by most as Γ and Γ_1 are denoted by some as Γ_1 and Γ_2 [30]. Also, Belin and Belin [31] use Γ to denote a $Fe_{13}Zn_{39}$ phase that we have not seen mentioned anywhere other than in their paper.

Of the 11 phases listed by Gosh, we could not find a crystal structure for the Γ_2 phase. Apart from literature we also consulted the Pearson's Crystal Data, Pauling File and AtomWork (MatNavi) databases. It would appear that the atomic structure is at present unknown. Also, it is too slow to form during hot dip galvanising [30] and is therefore less relevant. The Pauling File structure database has an entry for a 408 atom Γ_1 $Fe_{11}Zn_{40}$ structure, in which 48 lattice sites have a 2/3 chance of being occupied by Fe and 1/3 chance of being occupied by Zn. Sampling a number of different occupancies at high accuracy (to achieve absolute energy convergence between the very different crystal structures) to determine which ones have low energies, is beyond our computational means. With a unit cell of 556 atoms (52 Fe, 504 Zn), the δ phase is also still impractical to handle with DFT at high accuracy, though Belin and Belin [31] have carried out a Tight Binding calculation of it.

We are left with six FeAl and two FeZn intermetallics that can be calculated. Of these, the Γ Fe_3Zn_{10} phase has a number of lattice sites with mixed occupancy. The Pauling File structure database lists it as a structure with a 52 atom unit cell that includes eight sites that can be occupied by either Fe or Zn, in essentially three different ways. We have calculated all three of these. $FeAl_2$ has long been thought to have an 18 atom unit cell [32, 33] with ten Al atoms, five Fe atoms and three lattice sites with 0.5/0.5 occupation by Fe/Al (making it on average $Fe_{6.5}Al_{11.5}$ rather than $FeAl_2$). Since it is impossible to simulate a single unit cell with the average $Fe_{6.5}Al_{11.5}$ composition, we have sampled three occupations closest to the average composition on either side, i.e. Fe_6Al_{12} and Fe_7Al_{11}. Recently, Chumak *et al* [34] have stated that the $FeAl_2$ structure includes one extra atom. This revision appears not to be widely known and not to have been broadly accepted yet. At the time of writing up of our study, the paper reporting the structure redetermination has been cited only twice. While Mihalkovič and Widom [17] did a DFT calculation of the newly suggested $FeAl_2$ structure, we have chosen to calculate the long-accepted one.

The η Fe_2Al_5 phase consists of a 14 atom unit cell in which the four Fe and eight Al atoms form two 'tunnels'. In each of these tunnels one more Al atom can occupy one out of six different positions. We have relaxed three initial structures with the two Al 'tunnel atoms' occupying different combinations of positions in each tunnel. This resulted in two out of three structures relaxing towards the same minimum, giving us two different occupations.

Structure databases list intermetallics not present in the table listing intermetallics in FeZnAl by Gosh. These include the $FeAl_6$ phase, which is metastable and decomposes into $FeAl_3$ and Al. The Pauling file database lists an Al_2Zn phase, which is also not relevant for our work. We have not calculated either of these phases. Finally we mention two things to avoid possible confusion. First, while one of the FeAl intermetallics in our calculations is the η Fe_2Al_5 phase, it should be noted that hcp Zn with small amounts of Fe dissolved in it may be referred to as η-Zn. Second, while works that mention $FeAl_3$ may actually be talking about Fe_4Al_{13}, some DFT studies have looked at the 'mirror configuration' of the α_1 Fe_3Al phase, i.e. an actual $FeAl_3$ phase with the crystal structure of α_1 but with opposite Fe/Al occupation (see e.g. [10, 11]).

In order to get an impression of which phases are present at which temperature and over which composition ranges, fig. 1 shows the three binary phase diagrams, a section of the ternary phase diagram at 450 °C and a magnification of the Zn-rich corner of the ternary phase diagram at the same temperature.

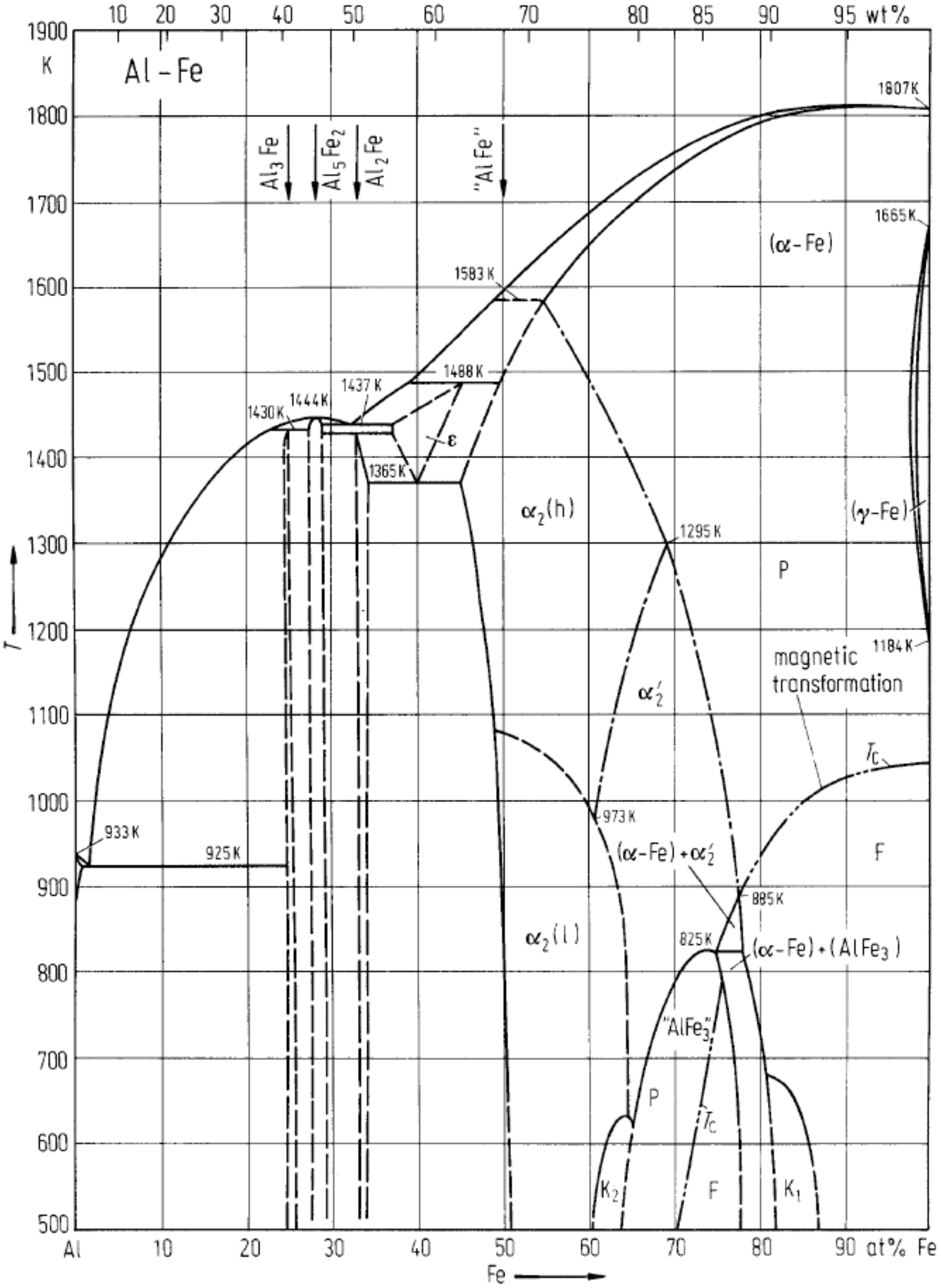

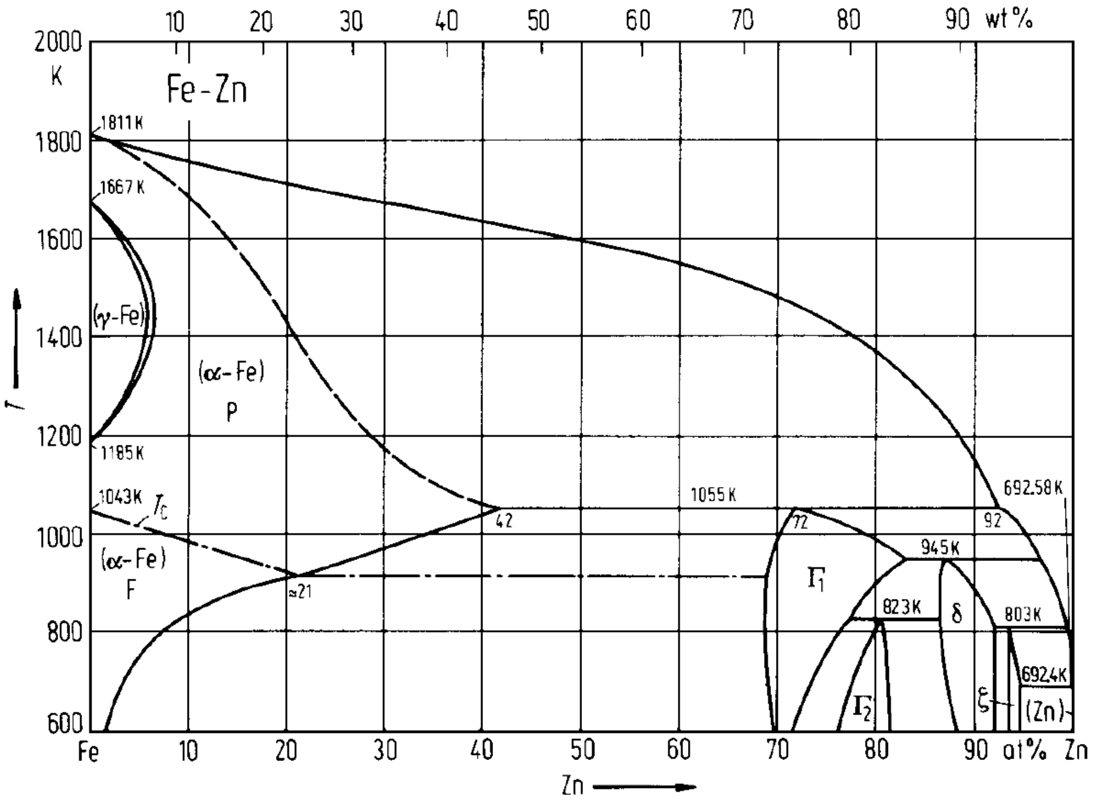
Fe-Zn
10 20 30 40 50 60 70 80 90 wt%
2000 K
1800
1600
1400
1200
1000
800
600
T
1811 K
1667 K
(γ-Fe)
(α-Fe) P
1185 K
1043 K
T_C
(α-Fe) F
42
≈21
1055 K
72
92
692.58 K
945 K
Γ_1
823 K
δ
803 K
692.4 K
Γ_2
ξ
(Zn)
Fe 10 20 30 40 50 60 70 80 90 at% Zn
Zn

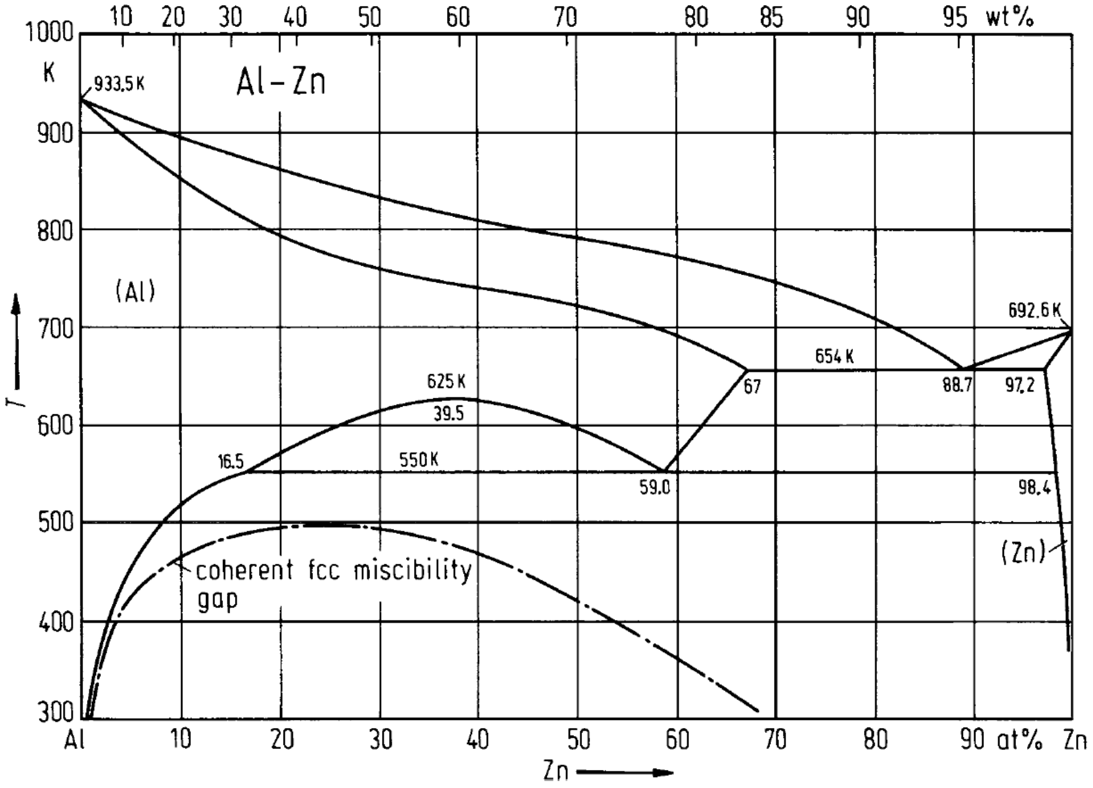
Al-Zn
10 20 30 40 50 60 70 80 85 90 95 wt%
1000 K
900
800
700
600
500
400
300
T
933.5 K
(Al)
692.6 K
654 K
67
88.7
97.2
625 K
39.5
16.5
550 K
59.0
98.4
(Zn)
coherent fcc miscibility gap
Al 10 20 30 40 50 60 70 80 90 at% Zn
Zn

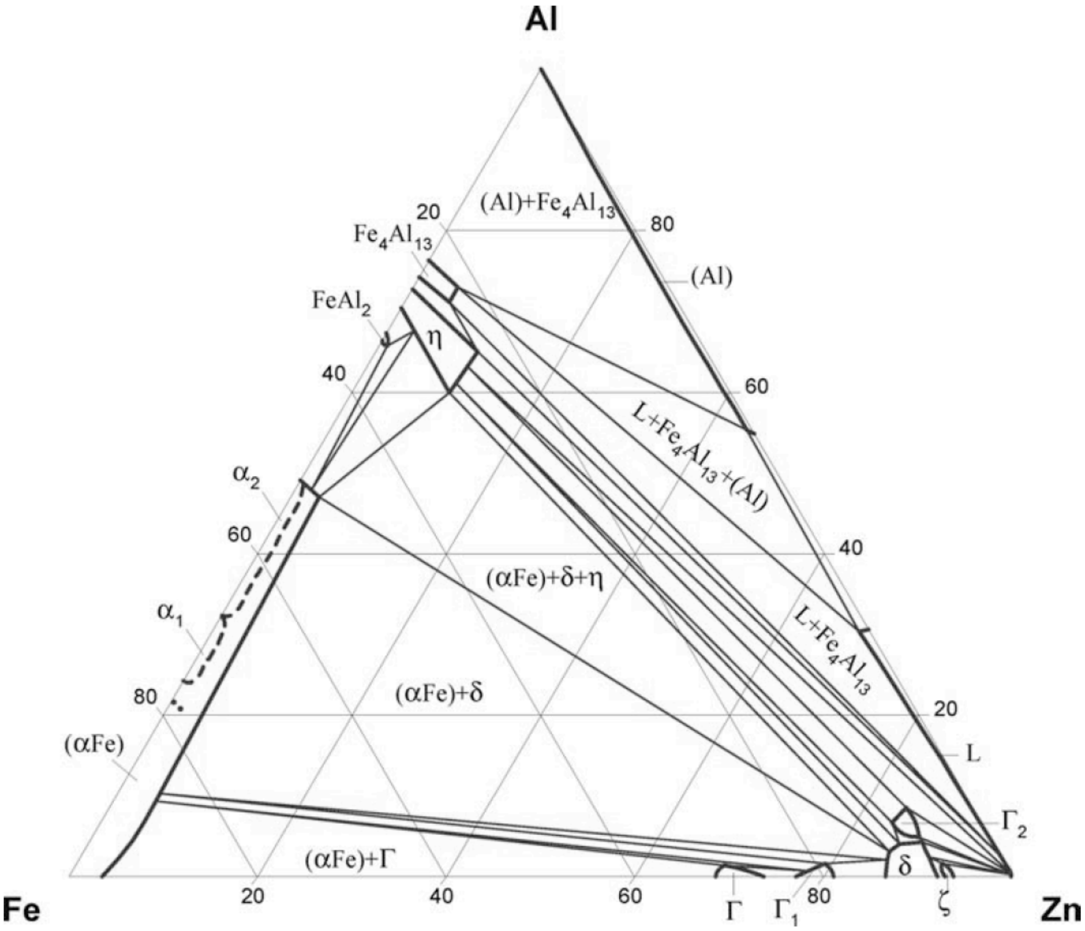

Al
(Al)+Fe_4Al_{13}
20
80
Fe_4Al_{13}
(Al)
$FeAl_2$
η
40
60
L+Fe_4Al_{13}+(Al)
α_2
60
40
(αFe)+δ+η
α_1
L+Fe_4Al_{13}
80
(αFe)+δ
20
(αFe)
L
Γ_2
(αFe)+Γ
δ
Fe
20
40
60
Γ
Γ_1
80
ζ
Zn

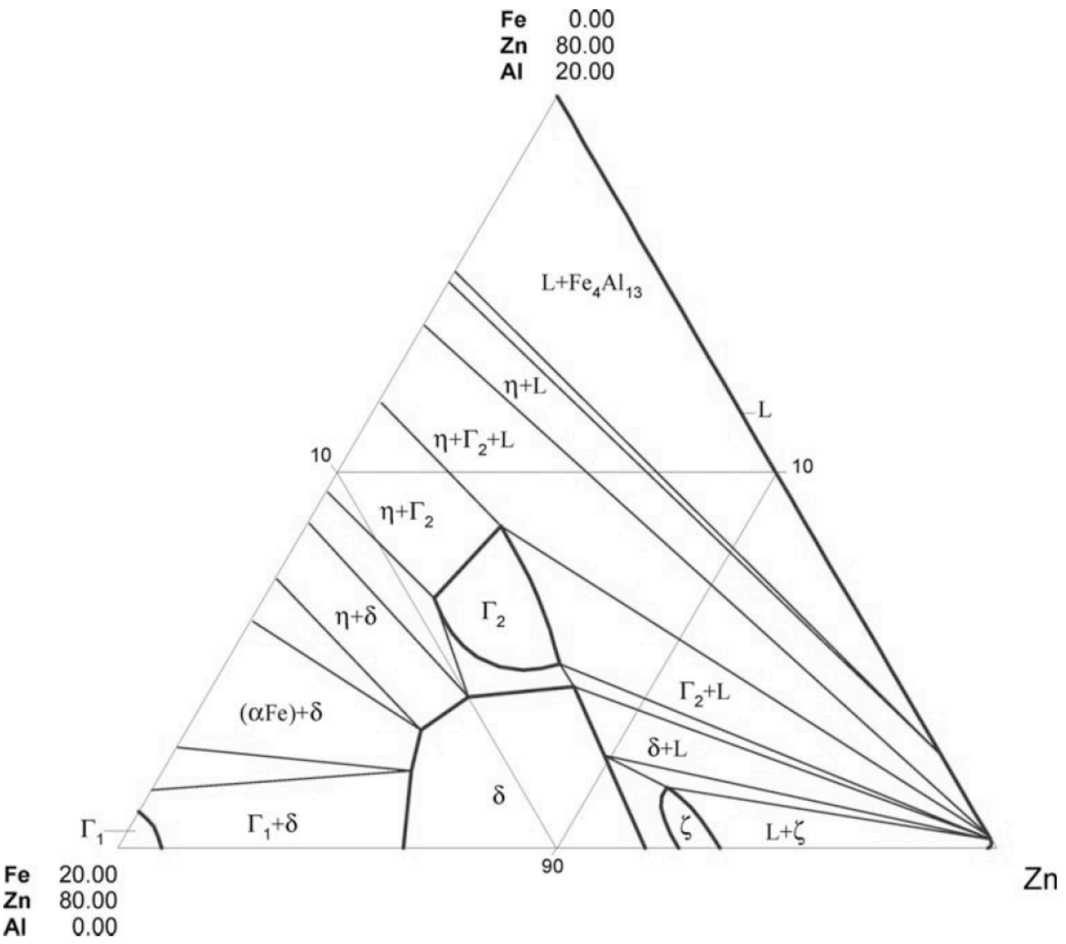

Figure 1. The FeAl (1A, [35]), FeZn (1B, [36]) and AlZn (1C, [37]) binary phase diagrams, a 450 °C section of the FeZnAl ternary phase diagram (1D, [27]) and a magnification of the Zn-rich corner of the ternary phase diagram at the same temperature (1E). While the binary phase diagrams are shown in weight percent, the ternary phase diagram and the magnification of the Zn-rich corner are shown in atom percent. Note that the phases denoted as Γ_1 and Γ_2 in the FeZn binary phase diagram are denoted as Γ and Γ_1 in the ternary phase diagram and the magnification of the Zn-rich corner (see comment about different naming conventions in the first paragraph of this section). With kind permission from Springer Science+Business Media: figs. 1 in [35, 36, 37] and figs. 10 and 11 in [27].

3.2. Geometries, formation energies, magnetism

For the eight intermetallics we calculated, the relaxed geometries, formation energies and magnetic states are noted in tables 1 – 3 and compared to values found in literature.

Table 1. Calculated relaxed geometries of FeAl and FeZn intermetallics. When two results or a range of results are reported for one phase, the results refer to different occupations, see section 3.1 on which systems were calculated. The number of occupations calculated with PBE and PBEsol was not always the same, a single value may be reported for one while a range of values is reported for the

other. Column 4 reports length ratios of the lattice spacings calculated with PBE and PBEsol. Most literature values are those cited by Ghosh [27], except for the ε Fe_5Al_8 phase [28] and the ζ phase, the latter being taken from the Pauling File database.

phase, unit cell	PBE geometry	PBEsol geometry	PBE/PBEsol length ratio	geometry, literature values
α_1 Fe_3Al_1 $Fe_{12}Al_4$	5.734 Å	5.660 Å	1.013	5.7886 - 5.793 Å
α_2 FeAl Fe_1Al_1	2.881 Å	2.845 Å	1.012	2.8976 - 2.9078 Å
ε Fe_5Al_8 $Fe_{20}Al_{32}$	8.800 Å	8.720 Å	1.009	8.9757 Å
$FeAl_2$	4.789 - 4.845 Å	4.743 Å	1.010	4.878 Å
$Fe_{6.5}Al_{11.5}$	6.368 - 6.373 Å	6.307 Å	1.010	6.461 Å
	8.548 - 8.606 Å	8.466 Å	1.010	8.800 Å
Fe_6Al_{12}	92.64 - 94.85°	95.02°		91.75°
	74.77 - 79.49°	76.86°		73.27°
	97.76 - 98.12°	98.13°		96.89°
Fe_7Al_{11}	4.650 - 4.705 Å	4.593 - 4.667 Å	1.008 - 1.012	
	6.366 - 6.442 Å	6.310 - 6.376 Å	1.009 - 1.012	
	8.549 - 8.566 Å	8.451 - 8.475 Å	1.011 - 1.012	
	95.24 - 95.95°	95.15 - 95.80°		
	77.44 - 78.01°	77.36 - 77.95°		
	98.61 - 100.83°	98.84 - 100.87°		
η Fe_2Al_5	7.395, 7.408 Å	7.332, 7.339 Å	1.009, 1.009	7.6559 Å
Fe_4Al_{10}	6.485, 6.438 Å	6.430, 6.388 Å	1.009, 1.008	6.4154 Å
	4.206, 4.095 Å	4.172, 4.065 Å	1.008, 1.007	4.2184 Å
	90.00, 90.00°	90.00, 90.00°		90°
	87.29, 90.00°	87.30, 90.00°		90°
	90.00, 90.00°	90.00, 90.00°		90°
Fe_4Al_{13}	15.419 Å	15.307 Å	1.007	15.492 Å
$Fe_{24}Al_{78}$	8.021 Å	7.956 Å	1.008	8.078 Å
	12.420 Å	12.332 Å	1.007	12.471 Å
	90.00°	90.00°		90.00°
	107.71°	107.75°		107.69°
	90.00°	90.00°		90.00°
Γ Fe_3Zn_{10} $Fe_{12}Zn_{40}$	8.979 - 8.986 Å	8.804 – 8.817 Å	1.019 - 1.020	8.9741 - 9.018 Å
ζ $FeZn_{13}$	10.783 Å	10.588 Å	1.018	10.6356 Å
Fe_2Zn_{26}	7.600 Å	7.441 Å	1.021	7.61 Å
	5.070 Å	4.970 Å	1.020	5.01321 Å
	90.00°	90.00°		90.00°
	100.64°	100.67°		97.798°
	90.00°	90.00°		90.00°

All structures were relaxed with experimentally reported structures as starting points. No calculation resulted in a transformation of the initial experimental structure into a different structure. Calculated lattice spacings differ from experiment by a few percent at most and lattice vector angles by a few degrees at most. As expected, the geometries for PBE parameterization are always slightly larger than for PBEsol, by 0.7 – 2.1 %. For pure bcc Fe, fcc Al and hcp Zn unit cells the PBE-PBEsol lattice parameter differences are 1.7, 0.6 and 1.9% respectively. The size differences of the intermetallics are well explained from the pure element size differences. The differences for Zn-rich intermetallics are the largest and are approximately as large as for pure Zn. The differences for Al-rich intermetallics are the smallest and are almost as small as for pure Al.

Table 2. Calculated formation energies of FeAl and FeZn intermetallics, compared to literature values. When two calculated results or a range of results are reported for one phase, the results refer to different occupations, see section 3.1 on which systems were calculated. The number of occupations calculated with PBE and PBEsol was not always the same, a single value may be reported for one while a range of values is reported for the other.

phase, unit cell	E_f, PBE (eV/atom)	E_f, PBEsol (eV/atom)	E_f, literature (eV/atom)
α_1 Fe_3Al_1 $Fe_{12}Al_4$	-0.199	-0.209	experiment: -0.15 - -0.32 [15, 18] DFT: -0.198 - -0.23 [18, 19, 10, 11, 17]
α_2 FeAl Fe_1Al_1	-0.331	-0.363	experiment: -0.25 - -0.42 [6, references in 13, 19] DFT: -0.32 - -0.42 [18, 19, 10, 11, 12, 17]
ε Fe_5Al_8 $Fe_{20}Al_{32}$	-0.282	-0.290	DFT: -0.286 [17]
$FeAl_2$ $Fe_{6.5}Al_{11.5}$ Fe_6Al_{12} Fe_7Al_{11}	-0.212 - -0.257 -0.225 - -0.228	-0.258 -0.232 - -0.236	DFT: -0.337 [17] CALPHAD: -0.31 [14]
η Fe_2Al_5 Fe_4Al_{10}	-0.297, -0.309	-0.309, -0.326	DFT: -0.349 [17] CALPHAD: -0.31 [14]
Fe_4Al_{13} $Fe_{24}Al_{78}$	-0.330	-0.345	DFT:-0.32 - -0.347 [16, 17] CALPHAD: -0.30 [14]
Γ Fe_3Zn_{10} $Fe_{12}Zn_{40}$	-0.029 - -0.033	-0.035 - -0.041	thermod. assessm.: -0.05 [20]
ζ $FeZn_{13}$ Fe_2Zn_{26}	-0.029	-0.040	thermod. assessm.: -0.03 [20]

A comparison between the formation energies of FeAl and FeZn compounds makes it abundantly clear why Fe aluminides would form a barrier film between the Fe object and the Zn bath, as Fe aluminide formation energies are an order of magnitude more negative than those of FeZn intermetallics. This picture is the same for PBE and PBEsol results, even though PBEsol results are systematically a bit more negative than the PBE results.

When comparing our results against the literature values we obtained, agreement is at least reasonable and in other cases very good, except for the $FeAl_2$ structure, see next. The agreement is as expected, as Colinet compared DFT and experimental formation energies for a range of intermetallics, and found mostly reasonable or good agreement [38]. It should be noted that our results represent 0 K formation energies while most experimental data represents enthalpies evaluated at room temperature or higher temperatures. This means that agreement may be slightly better or worse than indicated in table 2.

The formation energy we found for the $FeAl_2$ structure is somewhat less negative than both the DFT and CALPHAD values found in literature. Rather than seeing this as a problem in our DFT calculations, we think that the result gives further evidence for the newly proposed crystal structure for $FeAl_2$ by Chumak *et al* [34]. For structures without mixed occupation sites (i.e. where perfectly similar structures can be compared), our DFT results agree very closely with those of Mihalkovič and Widom [17], who used the same DFT code we used. Thus, there would appear to be a 0.1 eV/atom 0 K formation energy difference in favour of the newly proposed crystal structure. In addition to the XRD results by Chumak *et al*, these formation energy considerations also confirm the newly proposed structure.

It is also understandable from table 2 why the η Fe_2Al_5 phase, which usually forms first, would (partially) transform to α_2 FeAl after longer times, as more Fe becomes available through diffusion. In 1:1 Fe:Al ratio a large amount of energy is gained by transforming into the FeAl phase.

Table 3. Calculated magnetic moments on Fe atoms in FeAl and FeZn intermetallics, compared to moments and/or the magnetic state found in literature. When a range of results is reported for one phase, it refers to all the different atoms within different occupations sampled for that phase, see section 3.1 on which systems were calculated. For the α_1 and ε phases, the two numbers refer to the two inequivalent Fe sites.

phase, unit cell	moments on Fe, (μ_B), PBE	moments on Fe, (μ_B), PBEsol	moments on Fe, (μ_B), literature magnetic state
α_1 Fe_3Al_1 $Fe_{12}Al_4$	2.4, 1.9	2.4, 1.8	experim.: 2.14, 1.46 moments parallel [39] DFT: 2.39, 1.89, moments parallel [18] average: 1.96 [17]
α_2 FeAl Fe_1Al_1	0.8	0.7	experiment: paramagnetic, no local moment on Fe [40] DFT: 0.68

			[17]
ε Fe_5Al_8 $Fe_{20}Al_{32}$	1.9, 14 average: 1.7	1.8, 1.3 average: 1.6	exp: phase stable only at high temp. DFT: average 1.55 [17]
Fe_6Al_{12} Fe_7Al_{11}	0.0 – 2.4 0.9 – 2.3	0.1 – 1.8 0.3 – 2.2	experiment: 2.55, 2.5 spin glass [41, 42] incommensurate antiferromagnetism [43] paramagnet, 2.9 [44] DFT: average 1.59 [17]
η Fe_2Al_5 Fe_4Al_{10}	non-spin-polarised	non-spin-polarised	experiment: 0.73 [45] paramagnet, 0.7 [44] DFT: non-spin-pol. [17]
Fe_4Al_{13} $Fe_{24}Al_{78}$	non-spin-polarised	non-spin-polarised	experiment: 0.44 [45] DFT: non-spin-pol. [17]
Γ Fe_3Zn_{10} $Fe_{12}Zn_{40}$	1.9 – 2.6	1.6 – 2.5	exp. :non-magnetic [46]
ζ $FeZn_{13}$ Fe_2Zn_{26}	0.5	non-spin-polarised	exp. :non-magnetic [46]

The results in table 3 show several disagreements between our DFT results and experiments. There is good agreement in one case, i.e. the α_1 phase. In other cases, our DFT results show local moments on the Fe atoms when experiments do not show any, non-spin-polarised solutions are found when experiments show the presence of local moments on Fe atoms and when both DFT and experiments show moments on Fe atoms, the magnitude of the moments can differ substantially. The disagreement for $FeAl_2$ is irrelevant, as energy considerations (see table 2) have added to experimental evidence that the long-accepted crystal structure of $FeAl_2$ was not correct.

While the DFT results concerning magnetism are disappointing, this does not make all the work presented in this paper useless for our purposes, i.e. determining the formation energies with consistent settings to get an accurate ranking of the phase stabilities. It should be noted that the systems that converged to a non-spin-polarised solution were started from an initial configuration with magnetic moments on the atoms. Some of these systems converged to a non-spin-polarised solution only after a good number of ionic iterations, with the Fe atoms maintaining small magnetic moments during the first ionic iterations. The ‘reluctance’ to converge to a non-magnetic solution probably indicates that these systems would have magnetic solutions not much higher in energy, as was indeed found by others for some systems. While different parameterizations can lead to different magnetic states or different magnitude moments for the same supercell, the influence on the formation energy is modest. For the ζ $FeZn_{13}$ phase, even the difference between magnetic and non-magnetic states does not result in a large formation energy difference. We conclude that while obtaining the correct magnetic state is worthwhile in itself, obtaining a different magnetic state or different size moments need not be too important for our prime interest, i.e. the formation energies.

For systems that converged toward a solution with moments on Fe atoms, a parallel alignment of the moments was energetically the most favourable. For the ζ $FeZn_{13}$ phase the energy difference for anti-parallel alignment of the two Fe moments was less than 1 meV/atom, which is within the margin of error, but for other magnetic intermetallics the resulting energy difference for misaligned Fe spins was at least hundredths of eV/atom. While we did not calculate all aspects of the Γ_1 $Fe_{11}Zn_{40}$ phase, a small, less accurate calculation showed it also had large ferromagnetically aligned moments on the Fe atoms, in contradiction to experiment [46] as with the other FeZn intermetallics. Al atoms often had small magnetic moments that were anti-ferromagnetically aligned to the moments on Fe atoms.

For a pure Fe unit cell the moment on an Fe atom in a PBE calculation (2.20 μ_B) is 0.07μ_B larger than for the equivalent PBEsol calculation. For intermetallics that result in magnetic solutions, the difference in the total moment is not always close to the number of Fe atoms in the unit cell times 0.07 μ_B. So while size differences between PBE and PBEsol calculations were adequately explained from the pure element calculations, this is not the case for the magnetism. Moments in PBEsol calculations are consistently a bit smaller than in PBE calculations, presumably because the PBEsol parameterization results in smaller geometries and the moments on Fe atoms are reduced as volume is decreased. For the ζ $FeZn_{13}$ phase it even makes the difference between having local moments with PBE and none with PBEsol.

3.3 Solute atoms

Single solute atoms of Fe, Zn or Al were calculated in ‘large’ supercells of the other two elements with either the PBE or both the PBE and PBEsol parameterizations. For the Fe atom in Al, there were persistent ionic convergence problems using the PBE potential and hence for this system alone PW91 parameterisation was used. Results for heats of solution, nearest-neighbour strain around the solutes and the magnetic moments on the solutes are presented in tables 4-6.

Table 4. Solution energies of Fe, Al and Zn atoms in host lattices of the other two metals.

	solution energy, PBE (eV)	solution energy, PBEsol (eV)	solution energy, literature (eV)
$Fe_{249}Al_1$	-0.78	-0.81	
$Fe_{249}Zn_1$	0.30	0.32	
$Al_{255}Zn_1$	0.18	0.12	experiment: 0.18 extrapolation from [37 fig. 3]
$Al_{255}Fe_1$	-0.51		
$Zn_{215}Al_1$	0.21		
$Zn_{215}Fe_1$	0.23		experiment: 0.15 extrapolation from [36 fig. 5]

The literature values quoted are extrapolated from formation enthalpies determined at higher temperatures, 653 K for AlZn, 1066 K for ZnFe. Despite this difference, both the comparisons between DFT and experiment and between different DFT parameterizations indicate that the error bar on our results is some hundredths of eV.

The overall picture of the solution energies agrees well with the intermetallic formation energies: heats of solution of Fe in Al and *vice versa* are by far the most negative, while other solution energies are smaller in absolute value. They are also of opposite sign.

When Fe-in-Al or Al-in-Fe solutes are transformed into Fe_4Al_{13} or Fe_3Al_1, the formation energy changes are as follows with PBE:

$$\Delta E_f\left(4Al_{255}Fe_1 \rightarrow Fe_4Al_{13} + 1007Al\right) = \left(-0.330*17-4\times-0.51\right)/Fe_4Al_{13}$$

$$= 3.57eV,\ 0.21\ eV/atom$$

$$\Delta E_f\left(Fe_{249}Al_1 \rightarrow Fe_3Al_1 + 246Fe\right) = \left(-0.199*4--0.78\right)/Fe_3Al_1$$

.

$$= -0.02eV,\ -0.005\ eV/atom$$

The energy calculated for the first reaction above agrees with the phase diagram, fig. 1. It is energetically more favourable to form the Fe_4Al_{13} phase than it is to dissolve the equivalent number of Fe atoms into bulk Al. There is only a small formation energy difference between dissolving Al in Fe and forming the Fe_3Al_1 phase. Hence, temperature effects would determine whether an Fe-rich system would dissolve Al or would form the Fe_3Al_1 phase.

Table 5. Distance changes between Fe, Al and Zn solute atoms and nearest-neighbour host lattice atoms of the other two elements. A positive value means outward relaxation of the host atoms, a negative value means relaxation towards the solute atom.

	nearest neighbour distance change, PBE (%)	nearest neighbour distance change, PBEsol (%)	nearest neighbour distance change, literature (%)
$Fe_{249}Al_1$	1.7	2.0	
$Fe_{249}Zn_1$	1.6	1.8	
$Al_{255}Zn_1$	0.1	0.1	experim.: -0.3, -0.2 [47, 48]
$Al_{255}Fe_1$	-3.5		DFT: -3.22 - -4.2 [49, 50]
$Zn_{215}Al_1$	0.6, 1.0		
$Zn_{215}Fe_1$	-1.3, -5.8		

While our result for Fe in Al falls well within the range of DFT results found in literature, our result for Zn in Al disagrees with experiment, even in the sign of the nearest neighbour distance distortion. It would seem a little unlikely that a smaller atom like Zn would push out its larger Al neighbour atoms. We may therefore suspect that the error lies in our DFT result, though we have no good understanding as to why DFT calculations would fail in this instance. Also, it should be noted that a nearest-neighbour difference of tenths of a percent corresponds to only thousandths of an Ångström. While a wrong sign of the nearest neighbour distance distortion is a bad result, the magnitude of the error is quite small.

Except for the case of Zn in Al, all results can be understood from very simple atomic size considerations.

Table 6. Magnetic moments on Fe, Al and Zn solute atoms in host lattices of the other element(s). For Fe hosts, the Fe atoms have positive spin.

	moment on solute, PBE, (μ_B)	moment on solute, PBEsol, (μ_B)	moment on solute, literature, (μ_B)
$Fe_{249}Al_1$	-0.2	-0.2	DFT: -0.125 [51]
$Fe_{249}Zn_1$	-0.1		
$Al_{255}Fe_1$	1.2		experiment: 0 [52, 53] DFT: 0 – 1.63 [49, 50]
$Zn_{215}Fe_1$	1.6		experiment: 0 [52, 54] DFT: < 2.6, ≠ 0 [55]

As with the intermetallics, the magnetic results for solute systems are again the poorest, disagreeing with experiments in both cases where we found literature results. We note that other authors also reported DFT results with magnetic moments where experiments say there are none. As with FeAl intermetallics, for the Fe atom in Al the situation is quite subtle. Not allowing lattice relaxation results in the presence of a magnetic moment on the Fe atom in DFT calculations. However, allowing lattice relaxation slightly reduces the volume available to the Fe atom. Depending on the details of the DFT calculation, this can make the moment disappear. The relaxation energy is tiny, so as with FeAl intermetallics, the system appears to be near a tipping point where small changes can make the difference between a magnetic or non-magnetic solution. Erroneous magnetic results need not be make the results unusable if one is mostly interested in energies.

4 Summary

We have performed DFT calculation with two parameterizations, PBE and PBEsol, to determine the formation energies of FeAl and FeZn intermetallics. We have also determined the solution energies of Fe, Zn, and Al solutes in host lattices of the other two metals.
All fully relaxed geometries of the intermetallics are in good agreement with experimental results. As expected, PBEsol calculations result in slightly smaller geometries than PBE calculations. The differences vary from 0.7 – 2.1 % and are adequately explained from the PBE-PBEsol size differences of the pure elements. Formation energies fall within ranges of experimental results where available. They are either in excellent or at least reasonable agreement with other DFT results or CALPHAD or other thermodynamic assessments, except for the $FeAl_2$ phase, for which a structure revision was recently suggested. Comparison of our heat of formation result of the long-accepted structure to a DFT result for the newly suggested structure shows that the new structure is 0.1 eV/atom lower in energy than the established structure. Therefore energetic considerations also show that the new structure is indeed the correct one.
The formation energies show very clearly why Fe aluminides would form during galvanising in a Zn bath containing some Al, as Fe aluminides have formation energies an order of magnitude more negative than FeZn intermetallics. The results also show why the η Fe_2Al_5 phase that is quickest to form during galvanising, will transform into FeAl as more Fe becomes available with time. Fe_2Al_5 is 'wasteful' with Al, which can be used to produce more α_2 FeAl intermetallic as more Fe becomes available, while α_2 also has a more negative formation energy than Fe_2Al_5. PBEsol formation energies are a little more negative than equivalent PBE energies, but the overall picture for PBE and PBEsol results is still the same.
The calculated magnetic states of the intermetallics are most often wrong when compared to experiments. The magnetic states can be near tipping points where fine details of how the calculation is carried can make the difference between finding a magnetic or non-magnetic outcome. These details may include the DFT parameterisation, with the PBE calculation yielding a magnetic moment on Fe in ζ $FeZn_{13}$ while the PBEsol calculation turns to a non-spin-polarised solution. Still, while the wrong outcomes for the magnetic states are undesirable, the formation energies are not strongly affected.

In accordance with Fe aluminides having the most negative formation energies, the Fe/Al solute systems have the most negative solution energies. All other solution energies are positive and smaller in absolute value than the Fe/Al solution energies. Where literature values were found, DFT results and experiments differed by some hundredths of eV, the same difference as between DFT results based on different parameterisations.

The situation regarding magnetism of solute atoms is often also rather similar as in intermetallics. DFT results may disagree with experiment, but solute systems appear to be near tipping points and small changes in the calculations can make the difference between obtaining magnetic or non-magnetic outcomes. The energy differences between these outcomes are small.

Finally, lattice relaxation around solutes is mostly in line with a simple picture based on atomic sizes of the elements involved. One exception is the Zn solute in Al, which showed a small outward relaxation of the nearest neighbour Al atoms, at variance with experimental results.

Acknowledgements

Assistance from Rob Delhez and Ruud Hendrikx in searching crystallographic databases and thermodynamic data is gratefully acknowledged.

References

*klaver2@gmail.com

1 G. K. Mandal, D. Mandal, S. K. Das, R. Balasubramaniam, S. P. Mehrotra, Trans. Indian Inst. Met., **62** (2009) 35-40
2 M. Avettand-Fenoel, C. Cordier-Robert, G. Guillemot, F. Goodwin, J. Foct, Hyperfine Interact., **190** (2009) 29-36
3 A. R. Marder, Prog. Mater. Sc., **45** (2000) 191-271
4 P. Perrot, J. Tissier, J. Dauphin, Z. Metallkd., **83** (1992) 786-790
5 M. Potesser, T. Schoeberl, H. Antrekowitsch, J. Bruckner, EDP Congress 2006 (2006) 167-176
6 J. Breuer, A. Grün, F. Sommer, E. J. Mittemeijer, Metall. Mater. Trans. B, **32B** (2001) 913-918
7 V. Rohr, M. Schütze, E. Fortuna, D. N. Tsipas, A. Milewska, F. J. Pérez, Mater. Corros., **56** (2005) 874-881
8 S. C. Deevi, V. K. Sikka, C. T. Liu, Prog. Mater. Sc., **42** (1997) p177-192
9 P. Mohn, C. Persson, P. Blaha, K. Schwarz, P. Novák, H. Eschrig, Phys. Rev. Lett., **87** (2001) 196401
10 P. G. Gonzales-Ormeño, H. M. Petrilli, C. G. Schön, CALPHAD, **26** (2002) 573-582
11 N. Sodré, P. G. Gonzales-Ormeño, H. M. Petrilli, C. G. Schön, CALPHAD, **33** (2009) 576-583
12 J. Zou, C. L. Fu, Phys. Rev. B, **51** (1995) 2115-2121
13 K. Rzyman, Z. Moser, A. P. Miodownik, L. Kaufman, R. E. Watson, M. Weinert, CALPHAD, **24** (2000) 309-318
14 S. G. Fries, T. Jantzen, Thermochim. Acta, **314** (1998) 23-33
15 P. D. Desai, J. Phys. Chem. Ref. Data, **16** (1987) 109

16 C. Wolverton, Acta Mater., **49** (2001) 3129–3142
17 M. Mihalkovič, M. Widom, Phys. Rev. B, **85** (2012) 014113
18 P. Maugis, J. Lacaze, R. Besson, J. Morillo, Metall. Mater. Trans. A, **37A** (2006) 3397-3401
19 R. E. Watson and M. Weinert, Phys. Rev. B, **58** (1998) 5981-5988
20 G. Reumont, P. Perrot, J. M. Fiorani, J. Hertz, J. Phase Equilib., **21** (2000) 371-378
21 F. Lechermann, F. Welsch, C. Elsässer, C. Ederer, M. Fähnle, J. M. Sanchez, B. Meyer, Phys. Rev. B, **65** (2002) 132104
22 G. Kresse, J. Hafner, Phys. Rev. B, **47** (1993) 558-561
23 G. Kresse, J. Furthmuller, Phys. Rev. B, **54** (1996) 11169
24 P. E. Blöchl, Phys. Rev. B, **50** (1994) 17953
25 G. Kresse, D. Joubert, Phys. Rev. B, **59** (1999) 1758
26 J. P. Perdew, A. Ruzsinszky, G. I. Csonka, O. A. Vydrov, G. E. Scuseria, L. A. Constantin, X. Zhou, K. Burke, Phys. Rev. Lett., **100** (2008) 136406
27 G. Ghosh, *Aluminium – Iron – Zinc*. G. Effenberg and S. Ilyenko (ed.). The Landolt-Börnstein Database, Springer-Verlag Berlin Heidelberg, 2008. DOI 10.1007/978-3-540-69761-9_14
28 F. Stein, S.C. Vogel, M. Eumann, M. Palma, Intermetallics **18** (2010) 150-156
29 F. Zhou, Y. T. Chou, E. J. Lavernia, J. Mater. Res., **17** (2002) 3230-3236
30 V. Raghavan, J. Phase Equilib. Diffus., **29** (2008) 431-433
31 C. H. E. Belin, R. C. H. Belin, J. Sol. St. Chem., **151** (2000) 85-95
32 R. N. Corby, P. J. Black, Acta Cryst. C29 (1973) 2669-2677
33 A. M. van der Kraan, K. H. J. Buschow, Physica B, **138** (1986) 55-62
34 I. Chumak, K. W. Richter, H. Ehrenberg, Acta Cryst. **C66** (2010) i87–i88 Magnetic properties of FeAl2 and Fe2Al5
35 *Al-Fe (Aluminum-Iron)* in Landolt-Börnstein, Group IV: Physical Chemistry. Thermodynamic Properties. Phase Equilibria, Crystallographic and Thermodynamic Data of Binary Alloys · Ac-Au - Au-Zr, Springer-Verlag. DOI 10.1007/b20007, ISBN 978-3-540-15516-4
36 *Fe-Zn (Iron-Zinc)* in Landolt-Börnstein, Group IV: Physical Chemistry. Thermodynamic Properties. Phase Equilibria, Crystallographic and Thermodynamic Data of Binary Alloys · Dy-Er - Fr-Mo, Springer-Verlag. DOI 10.1007/b55397, ISBN 978-3-540-58428-5
37 *Al-Zn (Aluminum-Zinc)* in Landolt-Börnstein, Group IV: Physical Chemistry. Thermodynamic Properties. Phase Equilibria, Crystallographic and Thermodynamic Data of Binary Alloys · Ac-Au - Au-Zr, Springer-Verlag. DOI 10.1007/b20007, ISBN 978-3-540-15516-4
38 C. Colinet, Intermetallics **11** (2003) 1095-1102
39 R. Nathans, M. T. Pigott, C. G. Shull, J. Phys. Chem. Solids **6** (1958) 38-42
40 K. Miyatani, S. Iida, J. Phys. Soc. Jpn., **25** (1968) 1008-1016
41 C. S. Lue, Y. Öner, D. G. Naugle, J. H. Ross, Jr., Phys. Rev. B, **63** (2001) 184405
42 J. Chi, Y. Li, F. G. Vagizov, V. Goruganti, J. H. Ross, Jr., Phys. Rev. B, **71** (2005) 024431
43 D. Kaptás, E. Sváb, Z. Somogyvári, G. André, L. F. Kiss, J. Balogh, L. Bujdosó, T. Kemény, I. Vincze, Phys. Rev. B, **73** (2006) 012401
44 Z. Jagličić, S. Vrtnik, M. Feuerbacher, J. Dolinšek, Phys. Rev. B, **83** (2011) 224427

45 F. Müller, M. Rosenberg, W. Liu, U. Köster, Mater. Sci. Eng. A, **134** (1991) 900-903
46 J.-H. Hong, S.-J. Oh, S. J. Kwon, Intermetallics, **11** (2003) 207-213
47 U. Scheuer, B. Lengeler, Phys. Rev. B, **44** (1991) 9883-9894
48 J. Mimault, A. Fontaine, P. Lagarde, D. Raoux, A. Sadoc, D. Spanjaard, J. Phys. F, **11** (1981) 1311-1326
49 N. Papanikolaou, R. Zeller, P. H. Dederichs, N. Stefanou, Comp. Mater. Sci., **8** (1997) 131-135
50 F. Lechermann, M. Fähnle, B. Meyer, C. Elsässer, Phys. Rev. B, **69** (2004) 165116
51 G. Rahman, I. G. Kim, J. Magnetics, **16** (2011) 1-5
52 D. Riegel, L. Buermann, K. D. Gross, M. Luszik-Bhadra, S. N. Mishra, Phys. Rev. Lett., **61** (1988) 2192-2132
53 R. S. Preston, R. Gerlach, Phys.Rev. B, **3** (1971) 1519-1526
54 A. E. Bell, A. D. Caplin, J. Phys. F, **5** (1975) 143-152
55 P. G. Gonzales, L. A. Terrazos, H. M. Petrilli, S. Frota-Pessôa, Phys. Rev. B, **57** (1998) 7004-7009